TOXICOLOGICAL SCIENCES, 165(2), 2018, 447–461

doi: 10.1093/toxsci/kfy153
Advance Access Publication Date: June 22, 2018
Research Article

Aryl Hydrocarbon Receptor-Dependent Metabolism Plays a Significant Role in Estrogen-Like Effects of Polycyclic Aromatic Hydrocarbons on Cell Proliferation

Martina Hýžďalová,[*,†] Jakub Pivnička,[*,‡] Ondřej Zapletal,[*,‡] Gerardo Vázquez-Gómez,[*,§] Jason Matthews,[¶] Jiří Neča,[†] Kateřina Pěnčíková,[†] Miroslav Machala,[†] and Jan Vondráček[*,1]

[*]Department of Cytokinetics, Institute of Biophysics of the Czech Academy of Sciences, 61265 Brno, Czech Republic; [†]Department of Chemistry and Toxicology, Veterinary Research Institute, 62100 Brno, Czech Republic; [‡]Department of Experimental Biology, Faculty of Science, Masaryk University, 61137 Brno, Czech Republic; [§]Genomic Medicine and Environmental Toxicology Department, Instituto de Investigaciones Biomédicas, Universidad Nacional Autónoma de México C.U, 04510 Mexico City, Mexico; and [¶]Department of Nutrition, Institute of Basic Medical Sciences, University of Oslo, 0372 Oslo, Norway

[1]To whom correspondence should be addressed at Department of Cytokinetics, Institute of Biophysics of the Czech Academy of Sciences, Královopolská 135, 61265 Brno, Czech Republic. Fax: +420-541211293. E-mail: vondracek@ibp.cz.

ABSTRACT

Polycyclic aromatic hydrocarbons (PAHs) are widespread environmental contaminants that interact in a complex manner with both the aryl hydrocarbon receptor (AhR) and estrogen receptors (ER). Their potential endocrine-disrupting activities may depend on both inhibitory AhR-ER cross-talk and on AhR-dependent metabolic production of estrogenic PAH metabolites. Here, we analyzed the impact of AhR on estrogen-like effects of PAHs, such as benzo[*a*]pyrene (BaP), in particular, on control of cell cycle progression/cell proliferation. Using AhR knockout variant of estrogen-sensitive human breast cancer MCF-7 cells (MCF-7 AhR^{KO} cells), we observed that the AhR-dependent control of cytochrome P450 family 1 (CYP1) expression played a major role in formation of estrogenic BaP metabolites, most notably 3-OH-BaP, which contributed to the ER-dependent induction of cell cycle progression/cell proliferation. Both BaP metabolism and the BaP-induced S-phase transition/cell proliferation were inhibited in MCF-7 AhR^{KO} cells, whereas these cells remained sensitive towards both endogenous estrogen 17β-estradiol or hydroxylated BaP metabolites. BaP was found to increase the activity of ER-dependent luciferase reporter gene in wild-type MCF-7 cells; however, unlike its hydroxylated metabolite, BaP failed to stimulate luciferase activity in MCF-7 AhR^{KO} cells. Similarly, estrogen-like effects of other known estrogenic PAHs, such as benz[*a*]anthracene or 3-methylcholanthrene, were diminished in MCF-7 AhR^{KO} cells. Ectopic expression of human CYP1A1 and CYP1B1 enzymes partly restored both BaP metabolism and its effects on cell proliferation. Taken together, our data suggest that the AhR-dependent metabolism of PAHs contributes significantly to the impact of PAHs on cell proliferation in estrogen-sensitive cells.

Key words: aryl hydrocarbon receptor; polycyclic aromatic hydrocarbons; cytochrome P450 family 1; hydroxylated metabolites; estrogen receptor; cell cycle.

Polycyclic aromatic hydrocarbons (PAHs) are a large group of organic pollutants, widely distributed in the environment in form of complex mixtures, which are generally produced in incomplete combustion processes (Boström *et al.*, 2002). The toxic modes of action of PAHs include both their genotoxicity, linked with production of mutagenic metabolites forming covalent DNA adducts (Baird *et al.*, 2005), and a range of less defined non-genotoxic effects contributing to their toxicity, based, e.g., on the interactions of PAHs with specific intracellular receptors, such as the aryl hydrocarbon receptor (AhR) (Machala *et al.*, 2001; Vondráček *et al.*, 2017), nuclear receptors or interference with other intracellular signaling pathways (Hardonnière *et al.*, 2017; Zhang *et al.*, 2016). During recent years, an increasing attention has been paid to the impact of PAHs or their mixtures on receptors for steroid hormones, such as androgen receptor and, in particular, estrogen receptors (ER) (Zhang *et al.*, 2016).

Although a number of studies have indicated that PAHs may interfere with estrogenic signaling, the exact mechanisms of their action are still not fully clear. Several early studies have suggested that PAHs acting as relatively strong AhR ligands, such as benzo[*k*]fluoranthene, exert anti-estrogenic effects (Arcaro *et al.*, 1999; Chaloupka *et al.*, 1992). This has been attributed to the PAH-induced activation of the AhR and the subsequent inhibition of estrogenic signaling via inhibitory crosstalk between the AhR and ERα. The mechanisms underlying this cross-talk may include, e.g., interference of the AhR-controlled enzymes with endogenous estrogen metabolism, the AhR-induced ERα degradation, competition of the two receptors for common transcriptional co-activators, or, a direct inhibition of the ER-dependent transcription via the AhR binding to inhibitory dioxin responsive elements within promoter regions of ER-responsive genes (Matthews and Gustafsson, 2006; Safe and Wormke, 2003; Shanle and Xu, 2011). In contrast to the proposed anti-estrogenic action of PAHs, further studies have revealed that a number of PAHs, including, e.g., 3-methylcholanthrene, BaP, or benz[*a*]anthracene (BaA), exhibit direct or indirect estrogen-like effects in a variety of both *in vitro* and *in vivo* assays (Abdelrahim *et al.*, 2006; Gozgit *et al.*, 2004; Kummer *et al.*, 2008; Liu *et al.*, 2006; Plíšková *et al.*, 2005b; Shipley and Waxman, 2006; Swedenborg *et al.*, 2008; Vondráček *et al.*, 2002). A recent study screening the Tox21 10,000 compound library also identified PAHs as ERα agonists (Huang *et al.*, 2015). The estrogenic action of some AhR ligands, including PAHs, have been attributed to their direct binding to ERα (Abdelrahim *et al.*, 2006). However, others have reported that metabolites of some environmentally abundant PAHs, such as chrysene or BaP, and not the parent PAHs themselves, play a major role in ERα transactivation (Charles *et al.*, 2000; Fertuck *et al.*, 2001b; van Lipzig *et al.*, 2005). Therefore, PAH metabolism would play a major role in determination of effects of PAHs on endocrine system, as it may act in a cell-specific manner or produce PAH metabolites interacting with specific ER subtypes (Sievers *et al.*, 2013; Swedenborg *et al.*, 2008). However, most of the previous studies investigating the role of metabolism in anti-estrogenic or estrogenic action of PAHs have relied on the use of chemical inhibitors of cytochrome P450 family 1 (CYP1) activity or AhR antagonists, such as α-naphthoflavone or 3′, 4′-dimethoxyflavone, which may alter both the AhR activity and the action of estrogens (Charles *et al.*, 2000; Fertuck *et al.*, 2001b; Lam *et al.*, 2018). The complex nature of the interactions among ERα, AhR, and its transcriptional partner AhR nuclear translocator (ARNT) (Ahmed *et al.*, 2009; Beischlag and Perdew, 2005; Labrecque *et al.*, 2012; Ruegg *et al.*, 2008; Wihlen *et al.*, 2009) makes it difficult to understand the nature of interactions of PAHs with estrogenic signaling in a system, where chemical compounds interfere with various components constituting signaling pathways for ERs and AhR.

The recent advances of gene editing technologies made it possible to develop specific cell lines carrying single or multiple gene deletions. Recently, human breast cancer AhR knockout MCF-7 cells became available (Ahmed *et al.*, 2014). MCF-7 cell line represents the most frequently used model for studying the effects of PAHs on estrogen signaling, with a sufficient metabolic capacity to generate large quantities of PAH metabolites. This cell line has been successfully used to evaluate the impact of PAHs on ERα, using both reporter gene assays and endogenous responses of cells, such as regulation of ER-dependent cell cycle and proliferation, as relevant endpoints (Abdelrahim *et al.*, 2006; Fertuck *et al.*, 2001b; Plíšková *et al.*, 2005b; Vondráček *et al.*, 2002). BaP-resistant MCF-7 cells, which lost AhR responsiveness, have been also previously shown to be a useful tool to study the impact of environmental pollutants, such as dioxin, on ER activity (Moore *et al.*, 1994). Therefore, in the present study, we have employed the AhR knockout variant of MCF-7 cells, created via targeted AhR disruption (Ahmed *et al.*, 2014), in order to address the role of AhR in the effects of PAHs previously identified as estrogenic compounds on ER activation and/or on stimulation of ER-dependent cell cycle progression/cell proliferation. We primarily focused on discrimination between the effects of parent PAHs and their metabolites. Our present results suggest that, while PAHs have some limited effects on ER proliferative signaling, the AhR-dependent metabolism of PAHs via CYP1 enzymes (leading to production of estrogen-like active PAH metabolites) contributes significantly to their estrogen-like effects on cell proliferation.

MATERIALS AND METHODS

Chemicals. BaP and BaA were purchased from Fluka (Buchs, Switzerland) and Sigma-Aldrich (Prague, Czech Republic), respectively. 3-Methylcholanthrene (3MC) was from Santa Cruz Biotechnology (Santa Clara, California). BaP metabolite standards (BaP-r-7, t-8, t-9, c-10-tetrahydrotetrol(±) [BaP-tetrol I-1], BaP-r-7, t-8, t-9, t-10-tetrahydrotetrol(±) [BaP-tetrol I-2], BaP-r-7, t-8, c-9, t-10-tetrahydrotetrol(±) [BaP-tetrol II-1], BaP-trans-7, 8-dihydrodiol(±) [BaP-7, 8-DHD], BaP-trans-9, 10-dihydrodiol [BaP-9, 10-DHD], BaP-trans-4, 5-dihydrodiol(±) [BaP-4,5-DHD], BaP-3, 6-dione, BaP-1,6-dione, BaP-6,12-dione, 1-OH-BaP, 3-OH-BaP and 9-OH-BaP) were all obtained from the National Cancer Institute's Chemical Carcinogen Standard Reference Repository (Midwest Research Institute, Kansas City, Missouri). The identities and purities of all standards were established by high-performance liquid chromatography (HPLC). Ethyl acetate (p.a. ACS), methanol (p.a. ACS), and methanol (HPLC gradient grade) were all purchased from Merck (Darmstadt, Germany). 17β-Estradiol (E2; Sigma-Aldrich) was used as a positive control for all estrogenicity assays at the indicated concentrations. 2, 3, 7, 8-Tetrachlorodibenzo-*p*-dioxin (TCDD), purchased from Cambridge Isotope Laboratories (Andover, Massachusetts), was used as a model AhR agonist. 7α, 17β-[9-[(4,4,5,5,5-Pentafluoropentyl)sulfinyl]nonyl]estra-1,3,5(10)-triene-3,17-diol (ICI182,780; Tocris Bioscience, Bristol, UK), was used as ER antagonist. All test compounds were dissolved in DMSO (Merck) and the final concentration of the solvent in the experimental medium did not exceed 0.2% (v/v). All other reagents were obtained from Sigma-Aldrich, unless stated otherwise.

Cell lines and cultivation conditions. Human breast cancer MCF-7 wild-type (MCF-7 AhR wt) cells, obtained from American Type Culture Collection (ATCC, Rockville, Maryland) and MCF-7 AhR

knockout cells (MCF-7 AhR^{KO}), which were generated as described previously (Ahmed *et al.*, 2014) were cultivated in Dulbecco's modified Eagle's medium/nutrient mixture F-12 Ham (DMEM/F12, Gibco, Thermo Fisher Scientific, Waltham, Massachusetts) supplemented with 1% penicillin-streptomycin and 5% or 10% fetal bovine serum (FBS; v/v), respectively (Thermo Fisher Scientific). The cells were maintained at 37°C in 5% CO_2 and 95% humidity, and they were subcultured every 2–3 days, or, when they reached 80% confluency. MCF-7 BOS cells (Soto *et al.*, 1995), which were kindly provided by A. M. Soto (Tufts University, Boston, Massachusetts), were cultivated as the other MCF-7 variants. T47D human breast carcinoma cells, which were used for cloning of CYP1A1 and CYP1B1 expression vectors, were purchased from ATCC and cultured in DMEM/F12 supplemented with 10% FBS (v/v) and 1% penicillin-streptomycin. The cells were maintained at 37°C and 5% CO_2 and subcultured every 2–3 days, or, when they reached 80% confluency. The T47D.Luc cells, stably transfected with pEREtataLuc reporter construct (Legler *et al.*, 1999), were provided by BioDetection Systems BV (BDS, Amsterdam, The Netherlands). T47D.Luc cells were maintained and cultivated as described previously (Plíšková *et al.*, 2005a). For the experiments, all MCF-7 cell variants were seeded in phenol red-free DMEM/F12 medium (Thermo Fisher Scientific) supplemented with 5% FBS, and then synchronized using phenol red-free DMEM/F12, supplemented with 5% dextran/charcoal-treated FBS (experimental medium), for 48 h. The cells were then treated with indicated compounds dissolved in DMSO as described above.

Cloning of human CYP1A1 and CYP1B1 expression vectors. For RNA isolation, T47D cells were seeded in 6-well plates at a density of 300,000 cells per well. The following day, cells were treated with 10 nM TCDD for 24 h. Total RNA was isolated with RNeasy spin columns (Qiagen, Valencia, California). For cDNA synthesis, 2 μg of extracted RNA was reversed transcribed using SuperScriptII (Invitrogen, Carlsbad, California) and either CYP1A1 (5′-CAAA CTCGAG CTAAGAGCGCAGCTGCATTTGG-3′) or CYP1B1 (5′-CAAAGTCGACTTATTGGCAAGTTT CCTTGGCTTG-3′) reverse primer. The cDNAs were PCR amplified with the using gene-specific forward primers, CYP1A1 CAAAGGATCCA TGCTTTTCCCAATCTCCATGTCG or CYP1B1 CAAAGGATCCA TGGGCACCAGCCTCAGCCCGA and their respective reverse and Pfu Turbo (Stratagene). The restriction enzyme sites, BamHI and XhoI for CYP1A1 and BamHI and SalI for CYP1B1 are underlined. A 50 μl reaction contained 1× Pfu Turbo buffer and 0.2 units of Pfu Turbo polymerase (Sigma), 0.2 mM dNTPs, 0.2 μM of each primer and 5 μl of cDNA. PCR cycling conditions included an initial step of 5 min at 95°C that was followed by 35 cycles of 30 s at 95°C to denature DNA, 30 s at 59°C for primer annealing, and 72°C for 1 min for elongation. Following amplification, PCR products were resolved using 1% agarose gel electrophoresis followed by visualization with ethidium bromide. The bands were excised, the DNA was purified and cloned into BamHI and XhoI sites of pcDNA3.1 (Invitrogen).

Plasmid transfections. MCF-7 wt and MCF-7 AhR^{KO} cells were seeded at density of 35,000 per cm^2 in a 24-well plates in 1 ml of phenol red-free DMEM/F12 medium, without antibiotics, supplemented with 5% dextran/charcoal-treated FBS. After 24 h, cells were transiently transfected with 3× ERE TATA luc reporter construct (Hall and McDonnell, 1999) (from Addgene, Cambridge, Massachusetts,) and pRL-TK vector encoding *Renilla* luciferase (Promega, Madison, Wisconsin), as a transfection efficiency control. Transfections were carried out in a final volume of 500 μl of Opti-MEM medium (Thermo Fisher Scientific) containing 0.5 μg of pRL-TK and 0.5 μg of 3X ERE TATA luc constructs per well, and 2 μl of Lipofectamine 2000 transfection reagent (Thermo Fisher Scientific). After 6 h, the transfection mixture was replaced with phenol red-free DMEM-F12 supplemented with 1% penicillin/streptomycin and 5% dextran/charcoal-treated FBS. For transfections of pcDNA3.1, pcDNA3.1_hCYP1A1 and pcDNA3.1_hCYP1B1 vectors, we used identical transfection conditions, with final volumes and concentrations adapted to 12-well plates; cells were transfected either with 2 μg of pcDNA3.1 (control) or with 1 μg of both pcDNA3.1_hCYP1A1 and pcDNA3.1_hCYP1B1 plasmids.

Reporter gene assay. Cells were treated with DMSO (negative control), E2 (positive control), BaA, BaP, 3MC or 3-OH-BaP 24 h after transfection in experimental medium and then incubated for indicated time. Following the treatment, medium was aspirated, cells were washed with phosphate-buffered saline (PBS) and lysed with passive lysis buffer (Promega). Luciferase activity was then measured using the Dual-Luciferase Reporter Assay (Promega), according to the manufacturer's instructions, on LM-01T luminometer (Immunotech, Prague, Czech Republic). The firefly luciferase activity in each treatment was normalized to the corresponding *Renilla* luciferase activity and expressed relative to maximum E2-induced response. Determination of estrogenic activity of PAHs and hydroxylated BaP metabolites in T47D.Luc cells is described in detail in the legend to Supplementary Figure 4.

Cell cycle analysis. Cells were grown in experimental medium and then synchronized using phenol red-free DMEM/F12, supplemented with 5% dextran/charcoal-treated FBS (experimental medium) for 48 h, as indicated above. Cells were then treated with indicated compounds for 24 h, using DMSO and E2 as negative and positive controls, respectively. In experiments with ICI182,780, this was added 1 h before addition of test compounds. Following the treatment, cells were harvested by trypsinization, washed twice in PBS, and fixed in 70% ethanol. DNA was stained (37°C; 30 min) with Vindelov's solution (10 mM Tris buffer, pH 8; 0.7 mg/ml RNAse; 50 μg/ml propidium iodide; 0.1% Triton-X100). The DNA content was analyzed by flow cytometer (FACSCalibur, Becton Dickinson, San Jose, California; using 488 nm argon ion laser for excitation). A total of 15,000 events were acquired per each sample and the percentage of cells in the individual cell cycle phases was analyzed using ModFit 3.0 software (Verity Software House, Topsham, California). Single cells were identified and gated by pulse-code processing of the area and the width of the signal. Cell debris was excluded by using the forward scatter threshold.

WST-1 assay. MCF-7 wt and MCF-7 AhR^{KO} cells were seeded at density of 3,000 cells per well in 100 μl of experimental medium in 96-well cell culture plates. The cells were allowed to attach for 24 h and then synchronized for 48 h. Test compounds, DMSO (negative control) and E2 (positive control) were then added in 100 μl of experimental medium supplemented with 5% dextran/charcoal-treated FBS. Five days later, 10 μl of cell proliferation reagent WST-1 (Roche Diagnostics, Mannheim, Germany) were added into each well and cells were incubated with WST-1 in cultivation condition for another 3 h in case of MCF-7 wt cells or 24 h in case of MCF-7 AhR^{KO} cells, as these cells exhibited a slower rate of metabolism. Following the incubation, the absorbance of WST-1 product was measured with a microplate spectrophotometer at 450 nm. In order to confirm that WST-1 data

corresponded with actual cell numbers of MCF-7 AhR^{KO} cells, we further employed CyQUANT Cell Proliferation Assay (Thermo Fisher Scientific) using CyQUANT® GR dye, which detects cellular nucleic acids. Cells at the end of incubation period were stained according to the manufacturer's instructions and fluorescence measurements were made using a microplate reader with excitation at 485 nm and emission detection at 530 nm.

Measurement of 7-ethoxyresorufin-O-deethylase (EROD) activity. EROD activity in untreated or TCDD-treated MCF-7 wt and MCF-7 AhR^{KO} cells was measured as described previously (Kabátková *et al.*, 2015). Briefly, at the end of incubation period, cells were washed twice with cold PBS, lysed and resorufin production was then measured in 96-well plates. Each well contained 20 μl of cell lysate, 2 mM 3, 3′-methylene-bis(4-hydroxycoumarin) (Sigma-Aldrich) in 50 μl of Tris-sucrose buffer (pH 8.0), and 25 μl of 20 μM 7-ethoxyresorufin (Sigma-Aldrich). The plates were pre-incubated for 20 min at 37°C, and 25 μl of 1 mM NADPH solution were added per well, in order to start the reaction. Plates were then incubated for 1 h at 37°C and resorufin production was then measured in Fluostar Galaxy (BMG Labtech GmbH, Ortenberg, Germany) with an excitation at 530 nm and emission detection at 590 nm. Protein concentrations were estimated using the bicinchoninic acid method. The levels of EROD activity were expressed relative to maximum EROD induction induced by 10 nM TCDD in MCF-7 wt cells.

Real-time quantitative RT-PCR (qRT-PCR) analysis. MCF-7 wt and MCF-7 AhR^{KO} cells were grown in 35 mm diameter cell culture dishes in experimental medium in presence of 10 μM BaP. Cells were collected at indicated time points, washed twice with cold PBS and lysed with cell lysis buffer. In experiments employing transient transfection of hCYP1A1 and hCYP1B1 expression vectors in MCF-7 AhR^{KO} cells, the transfections were carried out 24 h before the collection of cells. Total RNA was isolated from cells using the NucleoSpin®RNA II purification kit (Macherey-Nagel, Düren, Germany). The amplification of the samples was carried out with Superscript III Platinum One-Step qRT-PCR kit (Invitrogen, Carlsbad, California). Primers and the respective probes were provided by Generi Biotech (Hradec Králové, Czech Republic) or Roche Diagnostics (Mannheim, Germany). qRT-PCR reactions were performed using RotorGene 6000 (Corbett Life Science, Qiagen) thermocycler. The sequences of primers and probes for human CYP1A1, CYP1B1, and TBP reference gene, as well as qRT-PCR conditions, have all been reported previously (Kabátková *et al.*, 2015).

Analysis of BaP metabolites. MCF-7 wt and MCF-7 AhR^{KO} cells were grown in 60 mm cell culture dishes in experimental medium. Following the incubation of cells with BaP, cells were washed twice with cold PBS, scraped into Eppendorf tubes, centrifuged and the cell pellets were stored at −80°C until further analysis. In the experiments employing transient transfection of hCYP1A1 and hCYP1B1 expression vectors into MCF-7 AhR^{KO} cells, the transfections were carried out 24 h before the onset of BaP treatment. Determination of BaP metabolites was then performed as described previously (Kabátková *et al.*, 2015). Briefly, cell pellets were extracted twice with 700 μl of ethyl acetate, combined extracts were dried under a stream of nitrogen, redissolved in 50 μl of methanol and aliquot of 10 μl was injected into the HPLC column. The Agilent 1200 chromatographic system (Agilent Technologies, Santa Clara, California) was used for the LC–MS/MS analyses, using the conditions described previously (Kabátková *et al.*, 2015). A triple quadrupole mass spectrometer Agilent 6410 Triple Quad LC/MS (Agilent Technologies) with an atmospheric pressure chemical ionization was used for detection of the analytes. The levels of BaP metabolites were normalized to protein concentrations estimated with the bicinchoninic acid method.

Western blotting. Whole cell lysates were prepared by washing the cells twice in PBS and then harvested in 90 μl cell lysis buffer (1% SDS, 10% glycerol, 100 mM Tris pH 7.4, 1 mM NaF, 1 mM Na_3VO_4, 1 mM PMSF). Cell lysates were sonicated and protein concentration was determined by using the bicinchoninic acid method. Samples were mixed with SDS loading buffer (240 mM Tris–HCl pH 6.8, 6% SDS, 0.02% bromophenol blue, 30% glycerol, 3% β-mercaptoethanol) and boiled for 10 min. Equal amounts (20–30 μg) of total protein were subjected to SDS-PAGE using 10% polyacrylamide gels and transferred to polyvinylidene fluoride membranes (PVDF; GE Healthcare, Little Chalfont, UK) in a buffer containing 192 mM glycine, 25 mM Tris, and 10% methanol. The membranes were blocked for 1 h in 5% powdered nonfat milk in wash buffer (0.05% Tween-20 in 20 mM Tris; pH 7.4; 100 mM NaCl). The following primary antibodies were used: rabbit anti-AhR (Biomol, Germany; #SA-210), mouse anti-β-actin (Sigma-Aldrich; #A1978), mouse anti-human cyclin A2 (Cell Signaling Technology, Danvers, Massachusetts; #4656) and rabbit anti-phospho-retinoblastoma protein (pRb; Ser807/811) (Cell Signaling Technology; #9308). The primary antibodies were incubated with the blots overnight at 4°C. After washing the membranes in wash buffer, secondary antibodies coupled to horseradish peroxidase (anti-mouse IgG [GE Healthcare; #NA931V] or anti-rabbit IgG [GE Healthcare; #NA934V]) were added for 2 h. Detection was performed with Clarity™ Western ECL Substrate (BIO-RAD, Prague, Czech Republic) according to manufacturer's instructions and visualized on X-ray films. The equal loading was verified by β-actin expression.

Statistical analyses. The data are presented the means ± SD of at least three independent experiments. Differences between the groups were calculated using one-way ANOVA. With all statistical analyses, an associated probability (p-value) of <5% was considered significant.

RESULTS

Inducibility of Both Expression and Activity of CYP1A1/1B1 Is Severely Limited in MCF-7 AhR^{KO} Cells

The loss of AhR expression in MCF-7 cells has been shown to significantly reduce basal levels of CYP1B1 and CYP1A1, as well as to prevent inducible expression of these principle enzymes involved in detoxification and metabolic activation of BaP or related PAHs (Ahmed *et al.*, 2014). In order to verify that the cells used in this study exhibit this phenotype, we first determined levels of AhR protein, inducibility of EROD activity and induction of CYP1A1/1B1 mRNAs in MCF-7 AhR^{KO} cells, and compared them with MCF-7 AhR wt cells. As shown in Figure 1, no AhR protein was detected in MCF-7 AhR^{KO} cells by Western blotting (Figure 1A) and TCDD failed to stimulate any detectable EROD activity in AhR knockout cells (Figure 1B). BaP, which was used as a model PAH in our study, induced both CYP1A1 and CYP1B1 mRNAs in MCF-7 AhR wt cells, in a time-dependent manner; however, no induction of either enzyme was observed in MCF-7 AhR^{KO} cells (Figure 1C). This indicated that MCF-7 AhR^{KO} cells do not possess enzymatic activity necessary for metabolism of PAHs.

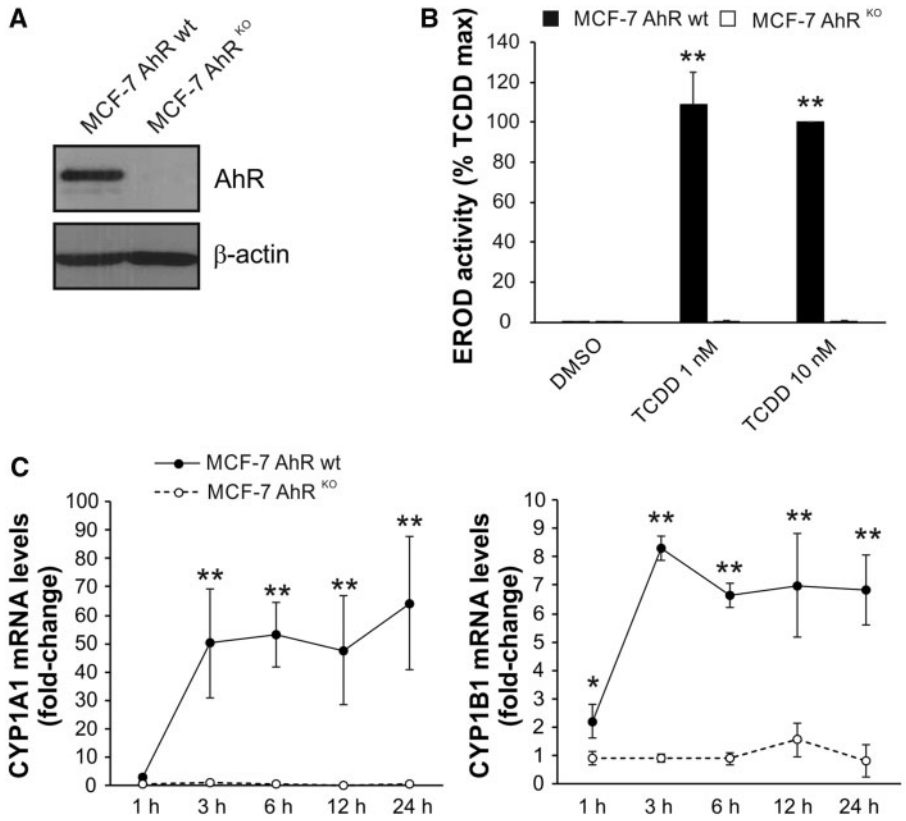

Figure 1. Lack of inducible CYP1A1 and CYP1B1 expression/activity in MCF-7 AhR^{KO} cells. A, MCF-7 AhR^{KO} cells were routinely monitored for the lack of AhR expression throughout the study. A representative result of Western blotting detection of AhR protein in MCF-7 AhR wt and MCF-7 AhR^{KO} cells is shown. B, TCDD failed to induce detectable 7-ethoxyresorufin-O-deethylase (EROD) activity in MCF-7 AhR^{KO} cells. Cells were incubated with DMSO (0.1%; negative control) or indicated concentrations of TCDD for 24 h and EROD assay was then performed as described in Materials and Methods. The results represent means ± SD of three independent experiments. Symbol "**" denotes significant difference ($p < 0.01$) between MCF-7 AhR wt and MCF-7 AhR^{KO} cells for the respective treatment group. C, BaP-induced CYP1A1 and CYP1B1 mRNA in MCF-7 AhR wt cells but not in MCF-7 AhR^{KO} cells. Cells were exposed to BaP (10 μM) for indicated time, lysed and total RNA was isolated. CYP1A1/1B1 mRNA levels were determined using qRT-PCR as described in Materials and Methods. The results represent means ± SD of three independent experiments. Symbol "*" denotes significant difference ($p < .05$) between MCF-7 AhR wt and MCF-7 AhR^{KO} cells at the respective time-point. Symbol "**" denotes significant difference ($p < .01$) between MCF-7 AhR wt and MCF-7 AhR^{KO} cells at the respective time point.

MCF-7 AhR^{KO} Cells Form Significantly Lower Levels of BaP Metabolites Than Parental Cells

Next, we evaluated the impact of the loss of AhR expression on metabolism of BaP in MCF-7 AhR^{KO} cells, as compared with wild-type cells. We incubated both cell lines with 10 μM BaP and collected them for analyses of BaP metabolites after 3, 6, and 24 h of exposure. As shown in Figure 2A, loss of AhR, which was associated with the lack of CYP1A1/1B1 expression/activity, severely limited formation of major BaP metabolites in MCF-7 AhR^{KO} cells. This was particularly evident at 24 h, where maximum levels of signature BaP metabolites, such as BaP-tetrols or BaP-DHDs, were several orders of magnitude higher in wild-type cells. Importantly, high levels of hydroxylated BaP metabolites, such as 1-, 3- and 9-OH-BaP, which have been shown to activate ER (Charles *et al.*, 2000; Fertuck *et al.*, 2001b; van Lipzig *et al.*, 2005), were only detected in MCF-7 AhR wt cells. Similar trends were observed also when we analyzed formation of BaP metabolites in MCF-7 cells treated with lower BaP concentrations (data not shown). In contrast, formation of BaP quinones, which are formed via radical cation pathway (Xue and Warshawsky, 2005), was less affected. Levels of BaP-6, 12-dione even slightly increased in knockout cells, thus indicating that some non-AhR-inducible enzymatic activity, perhaps masked by CYP1 enzymes in wild type cells, could be responsible for production of this BaP metabolite. Representative LC-MS/MS chromatograms showing profiles of major BaP metabolites in MCF-7 AhR^{KO} and MCF-7 AhR wt cells are shown in Figure 2B.

Induction of Cell Cycle Progression or Cell Proliferation PAHs Is Significantly Impaired in MCF-7 AhR^{KO} Cells

Next, we evaluated effects of two PAHs, BaA and BaP, which we have previously found to elicit estrogen-like effects on cell proliferation, in MCF-7 AhR wt and in MCF-7 AhR^{KO} cells (Plíšková *et al.*, 2005b; Vondráček *et al.*, 2002). First, we aimed to ascertain that endogenous estrogen, E2, stimulated cell cycle progression in MCF-7 AhR^{KO} cells in a similar manner as in wild-type cells. As shown in Supplementary Figure 1, E2 stimulated G_1-to-S-phase transition of MCF-7 AhR^{KO} cells, in a similar manner as in parental cell line or in MCF-7-BOS variant used for E-screen assay (Soto *et al.*, 1995). MCF-7 AhR^{KO} cells exhibited a better response to synchronization in dextran/charcoal-treated FBS, which might be the reason for lower percentage of S-phase found in control cells. Nevertheless, both cell lines exhibited a similar relative increase of percentage of cells in S-phase, which indicated that their proliferative responses to E2 remained comparable. In addition, we observed that E2 induced, in a dose-dependent manner, cell proliferation in both MCF-7 AhR wt and MCF-7 AhR^{KO} cells, as determined by WST-1 assay (Supplementary Figure 2), although reduction of WST-1 dye proceeded at a slower rate in MCF-7 AhR^{KO} cells (data not shown).

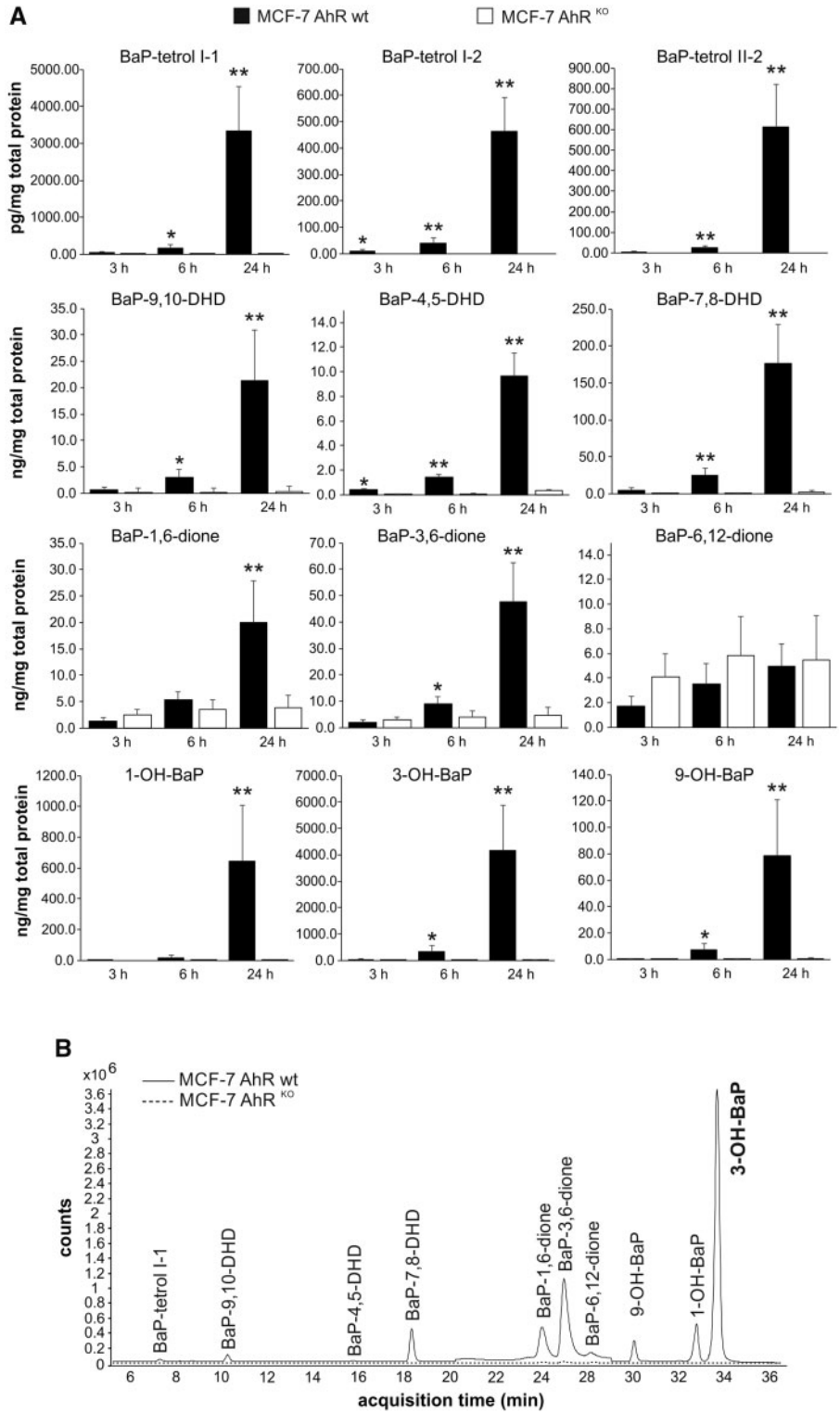

Figure 2. Lack of production of main BaP metabolites in MCF-7 AhR^{KO} cells. A, MCF-7 AhR wt cells (full bars) and MCF-7 AhR^{KO} cells (empty bars) were exposed to BaP (10 μM) and collected after indicated exposure times. BaP metabolites were extracted form cell pellets and analyzed by LC-MS/MS as described in Materials and Methods. Protein levels were estimated in parallel with metabolite detection, in order to allow normalization of results. The results represent means ± SD of three independent experiments. Symbol "*" denotes significant difference ($p < .05$) between MCF-7 AhR wt and MCF-7 AhR^{KO} cells at the respective time-point. Symbol "**" denotes significant difference ($p < .01$) between MCF-7 AhR wt and MCF-7 AhR^{KO} cells at the respective time-point. B, Representative LC-MS/MS chromatograms of BaP metabolites isolated from MCF-7 AhR wt (solid line) and MCF-7 AhR^{KO} (dashed line) cells exposed for 24 h to BaP (10 μM) are shown.

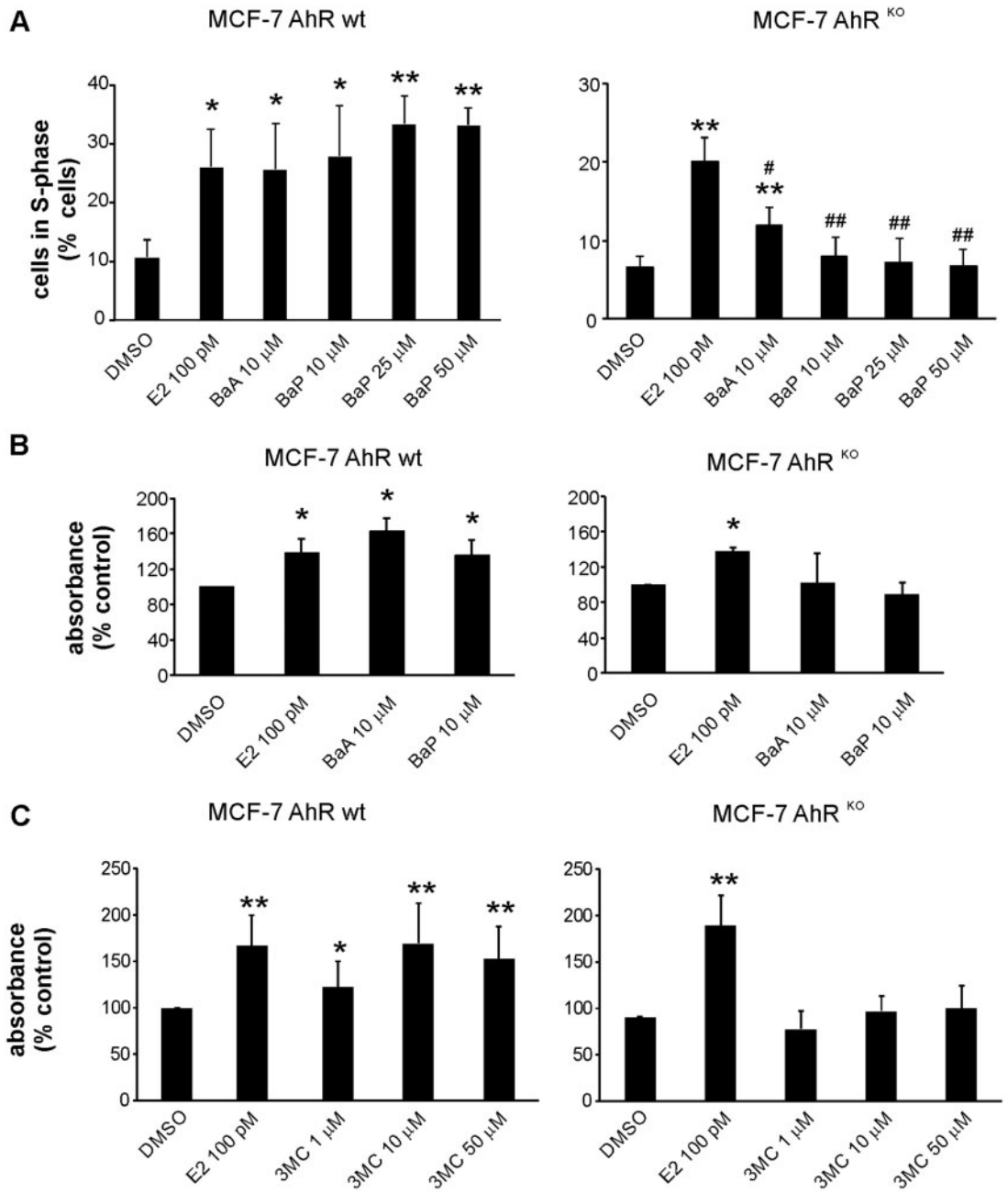

Figure 3. Effects of BaA and BaP on cell cycle progression and cell proliferation in MCF-7 AhR wt and MCF-7 AhR^{KO} cells. A, MCF-7 AhR wt and MCF-7 AhR^{KO} cells were synchronized in experimental medium (phenol red-free DMEM/F12, supplemented with 5% dextran/charcoal-treated FBS) for 48 h and then exposed to DMSO (0.1%; negative control), E2 (100 pM; positive control), BaA (10 μM), or BaP (10, 25, and 50 μM) for 24 h. Percentage of cells in S-phase was determined using flow cytometry as described in Materials and Methods. The results shown here represent means ± SD of three independent experiments. Symbol "*" denotes significant difference ($p < .05$), as compared with DMSO-treated cells. Symbol "**" denotes significant difference ($p < .01$), as compared with DMSO-treated cells. Symbol "#" denotes significant difference ($p < .05$), as compared to E2-treated cells. Symbol "##" denotes significant difference ($p < .01$), as compared to E2-treated cells. B, MCF-7 AhR wt and MCF-7 AhR^{KO} cells were synchronized in experimental medium for 48 h and then exposed to DMSO (0.1%; negative control), E2 (100 pM; positive control), BaA (10 μM), or BaP (10 μM) for 120 h. Cell proliferation was estimated using WST-1 assay as described in Materials and Methods. The results of absorbance detection were expressed relative to negative control (DMSO) and they represent means ± SD of three independent experiments. Symbol "*" denotes significant difference ($p < .05$), as compared to DMSO-treated cells. C, MCF-7 AhR wt and MCF-7 AhR^{KO} cells were cultured and treated as in (B). Cells were exposed to DMSO (0.1%; negative control), E2 (100 pM; positive control), or indicated concentrations of 3MC for 120 h. Cell proliferation was estimated using WST-1 assay as described in Materials and Methods. The results of absorbance detection were expressed relative to negative control (DMSO) and they represent means ± SD of three independent experiments. Symbol "*" denotes significant difference ($p < .05$), as compared with DMSO-treated cells. Symbol "**" denotes significant difference ($p < .01$), as compared with DMSO-treated cells.

These results confirmed that the loss of AhR did not block estrogen-like responses in MCF-7 cells.

Both BaA and BaP stimulated progression of cells into S-phase of cell cycle, and cell proliferation, in MCF-7 AhR wt cells (Figs. 3A and 3B). In contrast, we observed that in MCF-7 AhR^{KO} cells, induction of cell cycle progression by PAHs was significantly impaired (Figure 3A). Although a minor increase was observed for BaA, this was still lower than the effect of E2 in

MCF-7 AhR^{KO} cells. In contrast, in MCF-7 AhR wt cells, E2, BaA and BaP (up to 50 μM concentration) all induced a similar increase of percentage of cells in S-phase. Similar to that, induction of cell proliferation by BaA and BaP, as determined in WST-1 assay, was largely inhibited in MCF-7 AhR^{KO} cells (Figure 3B). Since we observed that the WST-1 reduction rate was slower in MCF-7 AhR^{KO} cells, we next verified our findings by using CyQUANT assay, which determines the levels of nucleic acids with a fluorescent dye. We found that although E2 (in a dose-dependent manner) significantly increased fluorescence in MCF-7 AhR^{KO} cells, the proliferative effects of both BaA and BaP were inhibited in cells lacking the AhR protein (Supplementary Figure 3). Finally, we used 3MC, as a model PAH which has been shown to directly activate ERα, to stimulate ERα-dependent transcription, and to increase uterine wet weight in a mouse assay *in vivo* (Abdelrahim *et al.*, 2006; Liu *et al.*, 2006). As shown in Figure 3C, 3MC stimulated cell proliferation in a dose-dependent manner (up to 50 μM concentration) in MCF-7 AhR wt cells. In contrast, its activity was inhibited in MCF-7 AhR^{KO} cells. Together, these results indicate that active metabolism of PAHs is important for cell proliferation induction, since in the absence of CYP1-dependent metabolism in MCF-7 AhR^{KO} cells, the proliferative effects of PAHs were largely inhibited.

PAHs Activate ER-Dependent Reporter Vector in MCF-7 AhR wt Cells, but Not in MCF-7 AhR^{KO} Cells

Since the results of proliferation assays indicated that a majority of estrogenic effects of PAHs depended on their CYP1-mediated metabolism, we next investigated their effects on ER transcriptional activity, using ER-dependent reporter gene. As shown in Figure 4A, PAHs increased, in a dose dependent manner, luciferase activity in MCF-7 AhR wt cells transiently transfected with reporter gene. BaA and BaP, at 10 μM concentration that was found to induce a maximum activity of AhR in human cell-based reporter assay (Vondráček *et al.*, 2017), did not inhibit the E2-induced reporter gene activity (Figure 4B). We then used MCF-7 AhR^{KO} cells, in order to measure effects of PAHs on activation of ER-dependent luciferase reporter, when their metabolism was compromised. As shown in Figure 4C (right), loss of the AhR-dependent CYP1 activity largely prevented activation of ER-dependent reporter vector in MCF-7 cells by BaA, BaP, or 3MC. We also observed only a low induction of luciferase activity in MCF-7 AhR wt cells after shorter 6 h incubation (Figure 4B), suggesting that lower levels of metabolites observed after shorter exposure (Figure 2A) may not be sufficient to elicit major estrogen-like response in MCF-7 cells.

3-OH-BaP, a Major BaP Metabolite Formed in MCF-7 Cells, Exhibits ER-Dependent Effects on Activation of ER-Dependent Reporter Gene and Cell Cycle Progression in MCF-7 AhR^{KO} Cells

The results of LC-MS/MS analyses indicated that 3-OH-BaP was the most abundant hydroxylated BaP metabolite formed in MCF-7 AhR wt cells. Both 3-OH-BaP and less abundant BaP metabolite, 9-OH-BaP, have been shown to be active in reporter gene and/or E-screen assays in MCF-7 cells (Charles *et al.*, 2000; Fertuck *et al.*, 2001b; van Lipzig *et al.*, 2005). We observed that 3-OH-BaP and 9-OH-BaP were indeed more potent inducers of ER-dependent reporter gene activity in stably transfected T47D.Luc cells than PAHs, including BaA, BaP, or 3MC (Supplementary Figure 4). As shown in Figure 4C (left), 3-OH-BaP stimulated the activity of ER-dependent reporter gene in a dose-dependent manner in MCF-7 AhR wt cells. Importantly, unlike parent PAHs, 3-OH-BaP also increased luciferase activity in a similar manner to E2 in MCF-7 AhR^{KO} cells (Figure 4C; right). Therefore, we hypothesized that this most abundant BaP metabolite identified in MCF-7 cells might play a role in stimulation of cell proliferation.

3-OH-BaP was found to induce cell cycle progression in both MCF-7 AhR wt and MCF-7 AhR^{KO} cells (Figure 5A), and the 3-OH-BaP-induced transition of cells into S-phase of cell cycle was prevented by synthetic anti-estrogen ICI182,780 (Figure 5A), thus confirming that it was ER dependent. 3-OH-BaP was also found to stimulate proliferation of MCF-7 AhR^{KO} cells, albeit to a lower extent than in parent MCF-7 AhR wt cells (Figure 5B). This might be attributed to its partial toxicity observed at higher doses. In addition, similar to 3-OH-BaP, the less abundant 9-OH-BaP was found to stimulate cell proliferation in MCF-7 AhR^{KO} cells (data not shown). Finally, we compared the effects of E2, BaP, and 3-OH-BaP on levels of two markers associated with progression of cells into S-phase: accumulation of cyclin A2 and phosphorylation of retinoblastoma protein (pRb) (Boylan *et al.*, 1999) in MCF-7 AhR^{KO} cells. As shown in Figure 5C, both E2 and 3-OH-BaP increased levels of cyclin A2 and phospho-pRb (Ser807/811), while BaP (at concentrations up to 25 μM) did not. Together, these results again suggested that metabolites of some PAHs may contribute significantly to their proliferative effects.

Transfection of MCF-7 AhR^{KO} Cells With hCYP1A1 and hCYP1B1 Partly Restores BaP Metabolism and Stimulation of Cell Cycle Progression

Since the above data indicated that metabolism of BaP plays a major role in its estrogen-like effects on cell proliferation, we next attempted to restore BaP metabolism in MCF-7 AhR^{KO} cells, using a transient expression of recombinant human CYP1A1/1B1 enzymes. As shown in Figure 6A, transient transfection with CYP1A1 and CYP1B1 expression vectors significantly increased levels of the respective RNAs in MCF-7 AhR^{KO} cells. We then determined levels of hydroxylated BaP metabolites (as well as level of BaP-7,8-DHD), in transfected cells exposed to BaP (10 μM), and we found that transfection with hCYP1A1 and hCYP1B1 expression vectors significantly increased formation of BaP metabolites as compared either with control cells or cells transfected with empty vector. Their levels were still lower than in parental cell line (Figs. 2A and 6B), which could be linked with lower levels of CYP1A1 and CYP1B1, when compared with AhR-ligand induced levels in MCF-7 AhR wt cells. We then evaluated effects of BaP on the stimulation of cell cycle progression in cells transfected with CYP1A1 and CYP1B1 expression vectors and compared it with control cells or cells transfected with empty pcDNA3.1 vector. We found that BaP significantly increased the percentage of S-phase cells in MCF-7 AhR^{KO} cells transfected with CYP1A1 and CYP1B1. In contrast, the presence or absence of CYP1 enzymes did not affect the E2-induced G_1-to-S-phase transition. These results suggested that metabolism contributed to the impact of BaP on cell cycle control in estrogen-sensitive MCF-7 cells.

DISCUSSION

A number of studies have proposed that individual PAHs and their complex mixtures, found in various environmental compartments or in tobacco smoke, may elicit estrogen-like responses in estrogen-sensitive cells or tissues (Charles *et al.*, 2000; Fertuck *et al.*, 2001a,b; Gozgit *et al.*, 2004; Kamiya *et al.*, 2005; Kummer *et al.*, 2008; Lam *et al.*, 2018; Liu *et al.*, 2006; Plíšková *et al.*, 2005b; Shipley and Waxman, 2006; Sievers *et al.*, 2013; Swedenborg *et al.*, 2008; Tsai *et al.*, 2004; van Lipzig *et al.*, 2005;

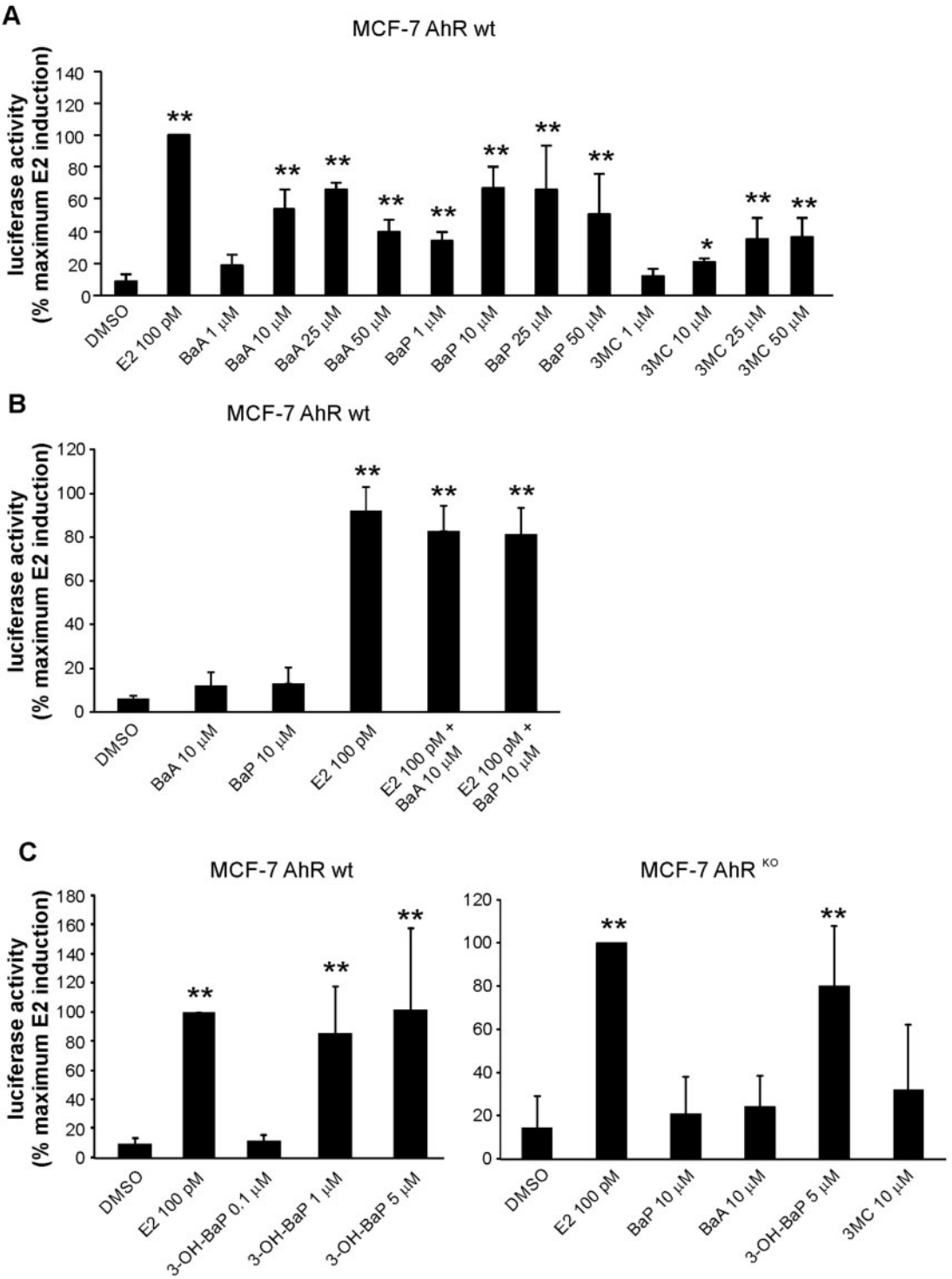

Figure 4. Effects of PAHs on induction of estrogen-dependent luciferase reporter gene in MCF-7 AhR wt and MCF-7 AhR^{KO} cells. A, MCF-7 AhR wt cells were grown in experimental medium for 24 h and then transiently transfected with 3X ERE TATA luc reporter construct and pRL-TK vector, encoding *Renilla* luciferase (transfection efficiency control). After 24 h of transfection, cells were exposed to DMSO (0.1%; negative control), E2 (100 pM; positive control), or indicated concentrations of PAHs for 24 h. Following the incubation, cells were collected, lysed and firefly/*Renilla* luciferase activities were determined with a luminometer. The results were expressed relative to maximum luciferase activity induced by reference compound (E2). B, MCF-7 AhR wt cells were grown in experimental medium for 24 h and then transfected with 3X ERE TATA luc reporter construct and pRL-TK vector as above. Aftere 24 h of transfection, cells were exposed to DMSO (0.1%; negative control), E2 (100 pM; positive control), BaA and BaP, or combinations of E2 and the respective PAH, for 6 h. Following the incubation, cells were collected, lysed, and firefly/*Renilla* luciferase activities were determined with a luminometer. C, MCF-7 AhR wt cells and MCF-7 AhR^{KO} cells were grown in experimental medium for 24 h and then transfected with 3X ERE TATA luc reporter construct and pRL-TK vector as above. After 24 h of transfection, MCF-7 AhR wt cells (left panel) were exposed to DMSO (0.1%; negative control), E2 (100 pM; positive control), or indicated concentrations of 3-OH-BaP for 24 h. MCF-7 AhR^{KO} cells (right panel) were exposed to DMSO, E2 or indicated concentrations of BaA, BaP, 3-OH-BaP, and 3MC for 24 h. Following the incubation, cells were collected, lysed, and firefly/*Renilla* luciferase activities were determined with a luminometer. All results were expressed relative to maximum luciferase activity induced by reference compound (E2). The results shown here represent means ± SD of three independent experiments. Symbol "*" denotes significant difference ($p < .05$), as compared with DMSO-treated cells. Symbol "**" denotes significant difference ($p < .01$), as compared with DMSO-treated cells.

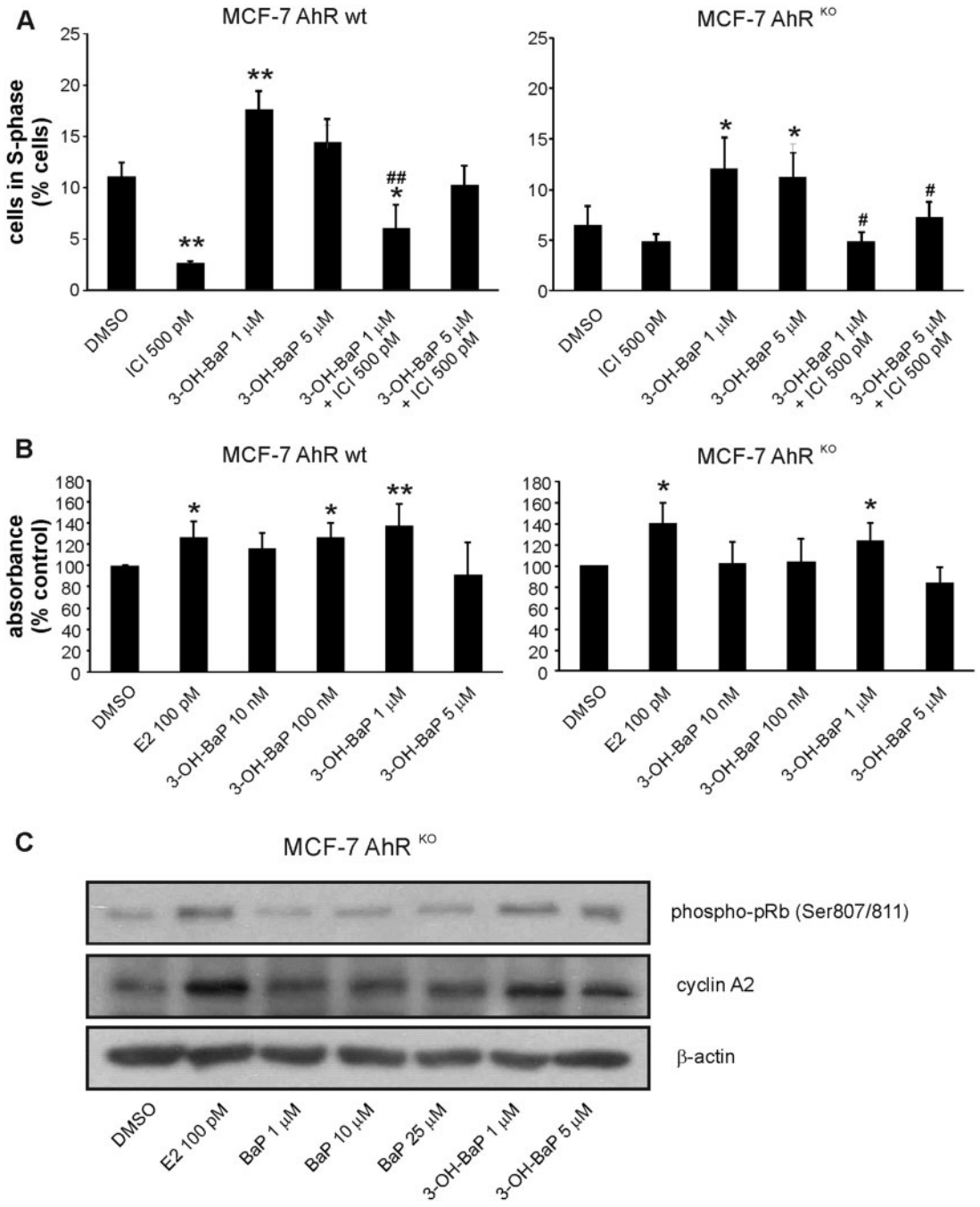

Figure 5. The major BaP metabolite identified in MCF-7 cells, 3-OH-BaP, induces estrogen-like effects on cell cycle progression and proliferation in MCF-7 AhR^{KO} cells. A, MCF-7 AhR wt and MCF-7 AhR^{KO} cells were synchronized in experimental medium (phenol red-free DMEM/F12, supplemented with 5% dextran/charcoal-treated FBS) for 48 h and then exposed to DMSO (0.1%; negative control) or indicated concentrations of 3-OH-BaP, alone, or in combination with synthetic ER antagonist, ICI 182,780 (ICI; 500 pM), for 24 h. Percentage of cells in S-phase was determined using flow cytometry as described in Materials and Methods. The results represent means ± SD of three independent experiments. Symbol "*" denotes significant difference ($p < .05$), as compared with DMSO-treated cells. Symbol "**" denotes significant difference ($p < .01$), as compared with DMSO-treated cells. Symbol "#" denotes significant difference ($p < .05$) between the respective 3-OH-BaP treatment group and its combination with ICI. Symbol "##" denotes significant difference ($p < .01$) between the respective 3-OH-BaP treatment group and its combination with ICI. B, MCF-7 AhR wt and MCF-7 AhR^{KO} cells were synchronized in experimental medium for 48 h and then exposed to DMSO (0.1%; negative control), E2 (100 pM; positive control), or indicated concentrations of 3-OH-BaP for 120 h. Cell proliferation was estimated using WST-1 assay as described in Materials and Methods. The results of absorbance detection were expressed relative to negative control (DMSO) and they represent means ± SD of three independent experiments. Symbol "*" denotes significant difference ($p < .05$), as compared with DMSO-treated cells. Symbol "**" denotes significant difference ($p < .01$), as compared with DMSO-treated cells. C, MCF-7 AhR^{KO} cells were synchronized in experimental medium for 48 h and then exposed to DMSO (0.1%; negative control), E2 (100 pM; positive control), or indicated concentrations of BaP and 3-OH-BaP for 24 h. Cells were collected, lysed, and protein levels of cyclin A2 and phosphorylated pRb (Ser 807/811) were determined by Western blotting. β-Actin was used as a loading control. The results shown here are representative of three independent experiments.

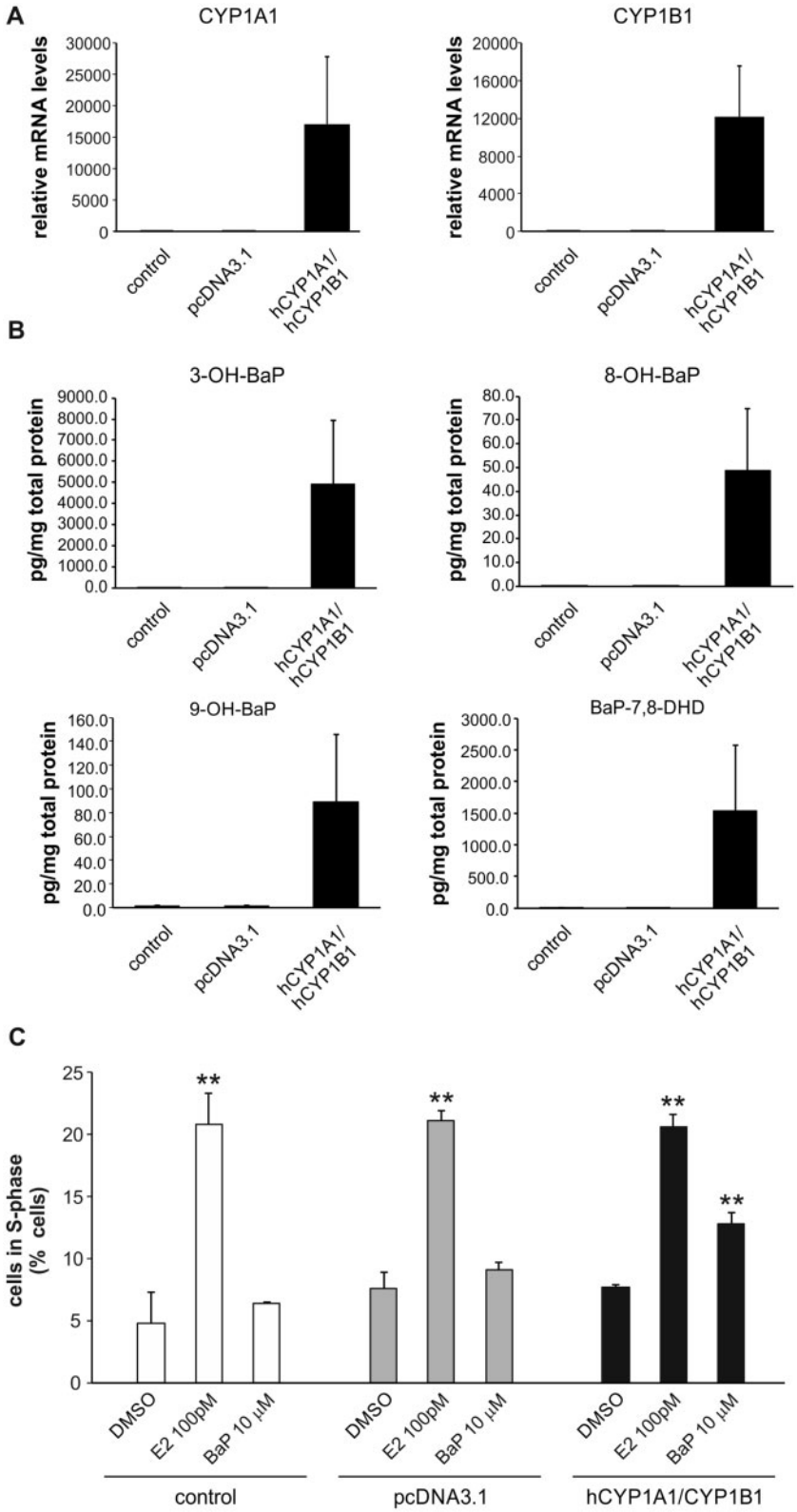

Figure 6. Transient transfection with human CYP1A1 and CYP1B1 enzymes restores both BaP metabolism and BaP-induced effects on cell cycle progression in MCF-7 AhR^{KO} cells. A, MCF-7 AhR^{KO} cells transiently transfected with empty vector (pcDNA3.1) or equal amount of hCYP1A1 and hCYP1B1 expression vectors and then cultivated for 24 h. Cells were then lysed and total RNA was isolated. CYP1A1/1B1 mRNA levels were determined using qRT-PCR as described in Materials and Methods. The results represent means ± SD of three independent experiments. B, MCF-7 AhR^{KO} cells transiently transfected with empty vector (pcDNA3.1) or equal amount of hCYP1A1 and hCYP1B1 expression vectors and then cultivated for 24 h. Cells were then exposed to BaP (10 μM) and collected after 24 h. BaP metabolites were extracted from cell pellets and analyzed by LC-MS/MS as described in Materials and Methods. Protein levels were estimated in parallel with metabolite detection, in order to allow normalization of results. The data represent means ± SD of three independent experiments. C, MCF-7 AhR^{KO} cells transiently transfected with empty vector (pcDNA3.1) or equal amount of hCYP1A1 and hCYP1B1 expression vectors and then cultivated for 24 h in experimental medium. Cells were then exposed to DMSO (0.1%; negative control), E2 (100 pM; positive control), or BaP (10 μM) for 24 h. Percentage of cells in S-phase was determined using flow cytometry as described in Materials and Methods. The results represent means ± SD of three independent experiments. Symbol "**" denotes significant difference ($p < .01$), as compared with the respective group of DMSO-treated cells.

Vondráček *et al.*, 2001, 2002; Zhang *et al.*, 2016). At the same time, many PAHs are also efficient AhR agonists, which control their own metabolism through AhR-dependent transcriptional regulation of CYP1 family enzymes (Nebert and Dalton, 2006). The activation of the AhR may then lead to formation of known estrogenic metabolites of PAHs (Charles *et al.*, 2000; Fertuck *et al.*, 2001b; Gozgit *et al.*, 2004; van Lipzig *et al.*, 2005), and it may elicit the inhibitory AhR-ERα cross-talk (Safe and Wormke, 2003). Some PAHs, such as 3MC, have been also found to activate ERα directly (Abdelrahim *et al.*, 2006). Loss of the AhR leads to dysregulation of ERα signaling in both male and female mice (Huang *et al.*, 2016), and the complex interactions of AhR and ER may contribute to adverse effects of contaminants in sensitive tissues, such as breast or lung epithelium (Helle *et al.*, 2016; Kuo *et al.*, 2013; Rodgers *et al.*, 2018). Both parent PAHs and their hydroxylated metabolites have also been shown to elicit developmental or endocrine-disrupting effects *in vivo* (Abdelrahim *et al.*, 2006; Booc *et al.*, 2014; Diamante *et al.*, 2017; Kummer *et al.*, 2008; Zhang *et al.*, 2016). It is thus important to better understand the mechanisms underlying the effects of PAHs on endocrine signaling at the cellular level, as many of the above studies often provide contradictory information about effects of PAHs on estrogen-dependent end-points (Zhang *et al.*, 2016). Therefore, given the highly complex nature of interactions between AhR and ERα, we examined the impact of PAHs on ERα signaling in the absence of the AhR-regulated metabolism of PAHs.

Using the MCF-7 AhR^{KO} cell line as a model, we found that these cells exhibit a near complete loss of both basal and inducible expression/activity of principle enzymes involved in metabolization of PAHs - CYP1A1 and CYP1B1. We used BaP as a model compound, since it has the best defined metabolism among PAHs with known estrogen-like effects (Xue and Warshawsky, 2005). We found that MCF-7 AhR^{KO} cells do not upregulate either CYP1 enzyme in response to BaP, and that they have only a very limited capacity to produce BaP metabolites, which was particularly relevant for hydroxylated metabolites of BaP, previously shown to activate ERα (Charles *et al.*, 2000; Fertuck *et al.*, 2001b; Gozgit *et al.*, 2004; van Lipzig *et al.*, 2005). The levels of 3-OH-BaP, a principal metabolite of BaP in MCF-7 AhR wt cells, were reduced by almost three orders of magnitude in MCF-7 AhR^{KO} cells, and a similar trend was observed also for other hydroxylated BaP metabolites. This corresponded with the observed disruption of CYP1 expression/activity in MCF-7 AhR^{KO} cell line. Importantly, MCF-7 AhR^{KO} cell line remained responsive to endogenous estrogens, such as E2, which both induced ER-dependent luciferase reporter gene and stimulated cell cycle progression/cell proliferation in AhR knockout cells. In addition, neither ERα levels nor induction of its binding to the regulatory regions of genes controlled by ERα (TFF1, GREB1) are affected by the absence of the AhR in this cell line (Ahmed *et al.*, 2014). This allowed us to examine the proliferative effects of PAHs in this cell model.

Cell proliferation or cell cycle progression is a well-defined end-point reflecting ERα activation in human estrogen-sensitive epithelial cell models (Miller *et al.*, 2016; Vanparys *et al.*, 2006), and we have therefore first focused on the impact of PAHs on proliferation in MCF-7 AhR^{KO} cells. When investigating the effects of BaP, we also included BaA as a second model estrogenic PAH, which is devoid of major genotoxic activity that might interfere with progression of cells through S-phase as previously shown in case of BaP (Plíšková *et al.*, 2005b). We found that both compounds stimulated progression of synchronized MCF-7 AhR wt cells into S-phase. In contrast, induction of cell cycle progression/cell proliferation was significantly inhibited in MCF-7 AhR^{KO} cells. This indicated that although BaA could, to some extent, stimulate cell cycle progression, a significant part of proliferative activities of both PAHs could be attributed to their metabolites. This is in agreement with the results of ERα-binding assays, where BaP did not bind directly the receptor (Fertuck *et al.*, 2001b; van Lipzig *et al.*, 2005). A possible weak binding activity of BaA seems to be in agreement with the observation that this PAH was found to be the most potent estrogenic PAHs (Huang *et al.*, 2015; Vondráček *et al.*, 2002). BaP and BaA did not inhibit ER-dependent activity of luciferase reporter gene in MCF-7 AhR wt cells, suggesting that they did not elicit inhibitory AhR-ERα cross-talk in MCF-7 cells. This is also supported by our observation that BaA and BaP did not inhibit the E2-induced cell cycle progression in wild-type cells (data not shown). 3MC stimulated cell proliferation in MCF-7 AhR wt cell cells but not in MCF-7 AhR^{KO} cells, thus indicating that although this PAH may activate ERα directly, its metabolites may also contribute significantly to its proliferative effects. Nevertheless, it should be noted that estrogen-like effects in various target cells/tissues may also vary depending on type of PAH or the studied endpoint, and in some cases, parent compound(s) are apparently effective as a direct ERα activator(s) (Abdelrahim *et al.*, 2006).

Similar to induction of cell proliferation, loss of the AhR in MCF-7 AhR^{KO} cells largely prevented activation of ER-dependent luciferase reporter gene by BaP, BaA, or 3MC. This seems to support the hypothesis that hydroxylated metabolites of both unsubstituted and substituted PAHs contributed significantly to their estrogen-like effects (Charles *et al.*, 2000; Fertuck *et al.*, 2001b; Lam *et al.*, 2017; van Lipzig *et al.*, 2005). Several hydroxylated metabolites of PAHs, including 2-, 3-, 8-, and 9-OH-BaP have been previously shown to stimulate cell proliferation or induction of ER-dependent reporter genes (Charles *et al.*, 2000; van Lipzig *et al.*, 2005). All four metabolites have been previously shown to have EC50 values lower than BaP in ER-CALUX assay or in MCF-7 cells (Charles *et al.*, 2000; van Lipzig *et al.*, 2005). This corresponded well with our own estimation of estrogenic EC50 values of 3-OH-BaP and 9-OH-BaP, which were within nanomolar range as compared with micromolar concentrations of parent PAHs, which were required to produce the same effect. Our LC-MS/MS analyses revealed that 3-OH-BaP was the principle hydroxylated BaP metabolite formed in MCF-7 cells. Therefore, we examined its ability to stimulate activation of ER-dependent reporter gene, cell cycle progression, or cell proliferation in both MCF-7 AhR wt and MCF-7 AhR^{KO} cells. We found that all three end-points were inducible by 3-OH-BaP, and that stimulation of cell cycle progression was fully repressed by synthetic estrogen ICI182,780, thus confirming that the proliferative effects of 3-OH-BaP were ER dependent. The effects on cell proliferation were also confirmed for another hydroxylated BaP metabolite, 9-OH-BaP (data not shown), which was nevertheless formed in significantly lower quantities in MCF-7 cells. 3-OH-BaP, but not BaP, was found to increase cyclin A2 protein levels and pRb phosphorylation in MCF-7 AhR^{KO} cells, two markers associated with progression of cells into S-phase (Boylan *et al.*, 1999). Together, this seems to imply that 3-OH-BaP was the principle estrogenic metabolite of BaP formed in MCF-7 cells, which mediated the estrogen-like action of its parent compound, BaP. Finally, we attempted to partially restore the BaP metabolism in MCF-7 AhR^{KO} cells through transient transfection with hCYP1A1 and hCYP1B1 enzymes. Transfection with CYP1 enzymes stimulated BaP metabolism and it partly restored formation of 3-OH-BaP as the most abundant BaP metabolite. This

was associated with a significant increase in percentage of cells entering S-phase (although lower than in case of E2). This again supports the hypothesis that metabolism of PAHs yields active hydroxylated metabolites, which in turn activate ERα, leading to the induction of ER-dependent cell proliferation in estrogen sensitive cells.

Activation of the AhR leading to repression of estrogen-regulated transcription has been shown to be an important toxic mode of action of persistent dioxin-like compounds, which might be independent of its transcriptional partner ARNT (Labrecque *et al.*, 2012; Matthews and Gustafsson, 2006; Safe and Wormke, 2003). However, both our present data and the previous studies summarized above indicate that the nature of interactions between the AhR and ERα could be more complex in case of readily metabolized AhR ligands, such as PAHs, which produce large quantities of estrogenic metabolites. The AhR-dependent metabolism of PAHs may significantly contribute to their impact on cell proliferation within estrogen-sensitive cells or tissues. In this context, it is perhaps interesting that estrogenic PAH metabolites can also be formed by human microbiota (Van de Wiele *et al.*, 2004), hydroxylated PAHs are found in cigarette smoke (Kamiya *et al.*, 2005) or that abundant alkylated PAHs may also form active estrogenic metabolites (Lam *et al.*, 2018). Polar compounds, including hydroxylated forms of polyaromatic compounds, could be also important contributors to estrogenicity of complex environmental mixtures (Lübcke-von Varel *et al.*, 2011). The present study thus contributes to a better understanding of mechanisms underlying the potential endocrine-disrupting activity of environmental PAHs and hydroxylated PAHs linked with ER activation.

SUPPLEMENTARY DATA

Supplementary data are available at *Toxicological Sciences* online.

ACKNOWLEDGMENTS

MCF-7 BOS cells were kindly provided by prof. Ana Soto (Tufts University, Boston, Massachusetts). T47D.Luc cells were kindly provided by BioDetection Systems BV (BDS, Amsterdam, The Netherlands). The expert technical assistance of Iva Lišková and Martina Urbánková is gratefully acknowledged.

FUNDING

This work was supported by the Czech Science Foundation [16-17085S to J.V.]. The institutional support of the Czech Academy of Sciences [to J.V.] and the Czech Ministry of Agriculture [RO 0517 to M.M.] is gratefully acknowledged. J.M. was supported by Canadian Institutes of Health Research (CIHR) operating grants (MOP-494265 and MOP-125919), an unrestricted research grant from the DOW Chemical Company, and the Johan Throne Holst Foundation.

REFERENCES

Abdelrahim, M., Ariazi, E., Kim, K., Khan, S., Barhoumi, R., Burghardt, R., Liu, S., Hill, D., Finnell, R., and Wlodarczyk, B. (2006). 3-Methylcholanthrene and other aryl hydrocarbon receptor agonists directly activate estrogen receptor alpha. *Cancer Res.* **66**, 2459–2467.

Ahmed, S., Valen, E., Sandelin, A., and Matthews, J. (2009). Dioxin increases the interaction between aryl hydrocarbon receptor and estrogen receptor alpha at human promoters. *Toxicol. Sci.* **111**, 254–266.

Ahmed, S., Wang, A., Celius, T., and Matthews, J. (2014). Zinc finger nuclease-mediated knockout of AHR or ARNT in human breast cancer cells abolishes basal and ligand-dependent regulation of CYP1B1 and differentially affects estrogen receptor alpha transactivation. *Toxicol. Sci.* **138**, 89–103.

Arcaro, K. F., O'Keefe, P. W., Yang, Y., Clayton, W., and Gierthy, J. F. (1999). Antiestrogenicity of environmental polycyclic aromatic hydrocarbons in human breast cancer cells. *Toxicology* **133**, 115–127.

Baird, W. M., Hooven, L. A., and Mahadevan, B. (2005). Carcinogenic polycyclic aromatic hydrocarbon-DNA adducts and mechanism of action. *Environ. Mol. Mutagen.* **45**, 106–114.

Beischlag, T. V., and Perdew, G. H. (2005). ER alpha-AHR-ARNT protein-protein interactions mediate estradiol-dependent transrepression of dioxin-inducible gene transcription. *J. Biol. Chem.* **280**, 21607–21611.

Booc, F., Thornton, C., Lister, A., MacLatchy, D., and Willett, K. L. (2014). Benzo[a]pyrene effects on reproductive endpoints in Fundulus heteroclitus. *Toxicol. Sci.* **140**, 73–82.

Boström, C. E., Gerde, P., Hanberg, A., Jernström, B., Johansson, C., Kyrklund, T., Rannug, A., Törnqvist, M., Victorin, K., and Westerholm, R. (2002). Cancer risk assessment, indicators, and guidelines for polycyclic aromatic hydrocarbons in the ambient air. *Environ. Health Perspect.* **110**, 451–488.

Boylan, J. F., Sharp, D. M., Leffet, L., Bowers, A., and Pan, W. (1999). Analysis of site-specific phosphorylation of the retinoblastoma protein during cell cycle progression. *Exp. Cell Res.* **248**, 110–114.

Chaloupka, K., Krishnan, V., and Safe, S. (1992). Polynuclear aromatic hydrocarbon carcinogens as antiestrogens in MCF-7 human breast cancer cells: role of the Ah receptor. *Carcinogenesis* **13**, 2233–2239.

Charles, G. D., Bartels, M. J., Zacharewski, T. R., Gollapudi, B. B., Freshour, N. L., and Carney, E. W. (2000). Activity of benzo[a]-pyrene and its hydroxylated metabolites in an estrogen receptor-alpha reporter gene assay. *Toxicol. Sci.* **55**, 320–326.

Diamante, G., do Amaral, E. S. M. G., Menjivar-Cervantes, N., Xu, E. G., Volz, D. C., Dias Bainy, A. C., and Schlenk, D. (2017). Developmental toxicity of hydroxylated chrysene metabolites in zebrafish embryos. *Aquat. Toxicol.* **189**, 77–86.

Fertuck, K. C., Kumar, S., Sikka, H. C., Matthews, J. B., and Zacharewski, T. R. (2001). Interaction of PAH-related compounds with the alpha and beta isoforms of the estrogen receptor. *Toxicol. Lett.* **121**, 167–177.

Fertuck, K. C., Matthews, J. B., and Zacharewski, T. R. (2001). Hydroxylated benzo[a]pyrene metabolites are responsible for in vitro estrogen receptor-mediated gene expression induced by benzo[a]pyrene, but do not elicit uterotrophic effects in vivo. *Toxicol. Sci.* **59**, 231–240.

Gozgit, J. M., Nestor, K. M., Fasco, M. J., Pentecost, B. T., and Arcaro, K. F. (2004). Differential action of polycyclic aromatic hydrocarbons on endogenous estrogen-responsive genes and on a transfected estrogen-responsive reporter in MCF-7 cells. *Toxicol. Appl. Pharmacol.* **196**, 58–67.

Hall, J. M., and McDonnell, D. P. (1999). The estrogen receptor beta-isoform (ERbeta) of the human estrogen receptor modulates ERalpha transcriptional activity and is a key regulator

of the cellular response to estrogens and antiestrogens. *Endocrinology* **140**, 5566–5578.

Hardonnière, K., Huc, L., Sergent, O., Holme, J. A., and Lagadic-Gossmann, D. (2017). Environmental carcinogenesis and pH homeostasis: not only a matter of dysregulated metabolism. *Semin. Cancer Biol.* **43**, 49–65.

Helle, J., Bader, M. I., Keiler, A. M., Zierau, O., Vollmer, G., Chittur, S. V., Tenniswood, M., and Kretzschmar, G. (2016). Cross-talk in the female rat mammary gland: influence of aryl hydrocarbon receptor on estrogen receptor signaling. *Environ. Health Perspect.* **124**, 601–610.

Huang, B., Butler, R., Miao, Y., Dai, Y., Wu, W., Su, W., Fujii-Kuriyama, Y., Warner, M., and Gustafsson, J. A. (2016). Dysregulation of notch and ERalpha signaling in AhR-/- male mice. *Proc. Natl. Acad. Sci. U. S. A.* **113**, 11883–11888.

Huang, R., Sakamuru, S., Martin, M. T., Reif, D. M., Judson, R. S., Houck, K. A., Casey, W., Hsieh, J. H., Shockley, K. R., Ceger, P., *et al.* (2015). Profiling of the Tox21 10K compound library for agonists and antagonists of the estrogen receptor alpha signaling pathway. *Sci. Rep.* **4**, 5664.

Kabátková, M., Zapletal, O., Tylichová, Z., Neča, J., Machala, M., Milcová, A., Topinka, J., Kozubík, A., and Vondráček, J. (2015). Inhibition of beta-catenin signalling promotes DNA damage elicited by benzo[a]pyrene in a model of human colon cancer cells via CYP1 deregulation. *Mutagenesis* **30**, 565–576.

Kamiya, M., Toriba, A., Onoda, Y., Kizu, R., and Hayakawa, K. (2005). Evaluation of estrogenic activities of hydroxylated polycyclic aromatic hydrocarbons in cigarette smoke condensate. *Food Chem. Toxicol.* **43**, 1017–1027.

Kummer, V., Mašková, J., Zralý, Z., Neča, J., Šimečková, P., Vondráček, J., and Machala, M. (2008). Estrogenic activity of environmental polycyclic aromatic hydrocarbons in uterus of immature Wistar rats. *Toxicol. Lett.* **180**, 212–221.

Kuo, L. C., Cheng, L. C., Lin, C. J., and Li, L. A. (2013). Dioxin and estrogen signaling in lung adenocarcinoma cells with different aryl hydrocarbon receptor/estrogen receptor alpha phenotypes. *Am J Respir. Cell Mol. Biol.* **49**, 1064–1073.

Labrecque, M. P., Takhar, M. K., Hollingshead, B. D., Prefontaine, G. G., Perdew, G. H., and Beischlag, T. V. (2012). Distinct roles for aryl hydrocarbon receptor nuclear translocator and Ah receptor in estrogen-mediated signaling in human cancer cell lines. *PLoS One* **7**, e29545.

Lam, M. M., Engwall, M., Denison, M. S., and Larsson, M. (2018). Methylated polycyclic aromatic hydrocarbons and/or their metabolites are important contributors to the overall estrogenic activity of polycyclic aromatic hydrocarbon-contaminated soils. *Environ. Toxicol. Chem.* **37**, 385–397.

Legler, J., van den Brink, C. E., Brouwer, A., Murk, A. J., van der Saag, P. T., Vethaak, A. D., and van der Burg, B. (1999). Development of a stably transfected estrogen receptor-mediated luciferase reporter gene assay in the human T47D breast cancer cell line. *Toxicol. Sci.* **48**, 55–66.

Liu, S., Abdelrahim, M., Khan, S., Ariazi, E., Jordan, V. C., and Safe, S. (2006). Aryl hydrocarbon receptor agonists directly activate estrogen receptor alpha in MCF-7 breast cancer cells. *Biol. Chem.* **387**, 1209–1213.

Lübcke-von Varel, U., Machala, M., Ciganek, M., Neca, J., Pencikova, K., Palkova, L., Vondracek, J., Löffler, I., Streck, G., Reifferscheid, G., *et al.* (2011). Polar compounds dominate in vitro effects of sediment extracts. *Environ. Sci. Technol.* **45**, 2384–2390.

Machala, M., Vondráček, J., Bláha, L., Ciganek, M., and Neča, J. (2001). Aryl hydrocarbon receptor-mediated activity of mutagenic polycyclic aromatic hydrocarbons determined using in vitro reporter gene assay. *Mutat. Res.* **497**, 49–62.

Matthews, J., and Gustafsson, J. A. (2006). Estrogen receptor and aryl hydrocarbon receptor signaling pathways. *Nucl. Recept. Signal.* **4**, e016.

Miller, M. M., Alyea, R. A., LeSommer, C., Doheny, D. L., Rowley, S. M., Childs, K. M., Balbuena, P., Ross, S. M., Dong, J., Sun, B., *et al.* (2016). Development of an in vitro assay measuring uterine-specific estrogenic responses for use in chemical safety assessment. *Toxicol. Sci.* **154**, 162–173.

Moore, M., Wang, X., Lu, Y. F., Wormke, M., Craig, A., Gerlach, J. H., Burghardt, R., Barhoumi, R., and Safe, S. (1994). Benzo[a]pyrene-resistant MCF-7 human breast cancer cells. A unique aryl hydrocarbon-nonresponsive clone. *J. Biol. Chem.* **269**, 9. 11751.

Nebert, D. W., and Dalton, T. P. (2006). The role of cytochrome P450 enzymes in endogenous signalling pathways and environmental carcinogenesis. *Nat. Rev. Cancer* **6**, 947–960.

Plíšková, M., Vondráček, J., Canton, R. F., Nera, J., Kočan, A., Petrík, J., Trnovec, T., Sanderson, T., van den Berg, M., and Machala, M. (2005a). Impact of polychlorinated biphenyls contamination on estrogenic activity in human male serum. *Environ. Health Perspect.* **113**, 1277–1284.

Plíšková, M., Vondráček, J., Vojtěšek, B., Kozubík, A., and Machala, M. (2005b). Deregulation of cell proliferation by polycyclic aromatic hydrocarbons in human breast carcinoma MCF-7 cells reflects both genotoxic and nongenotoxic events. *Toxicol. Sci.* **83**, 246–256.

Rodgers, K. M., Udesky, J. O., Rudel, R. A., and Brody, J. G. (2018). Environmental chemicals and breast cancer: an updated review of epidemiological literature informed by biological mechanisms. *Environ. Res.* **160**, 152–182.

Ruegg, J., Swedenborg, E., Wahlstrom, D., Escande, A., Balaguer, P., Pettersson, K., and Pongratz, I. (2008). The transcription factor aryl hydrocarbon receptor nuclear translocator functions as an estrogen receptor beta-selective coactivator, and its recruitment to alternative pathways mediates antiestrogenic effects of dioxin. *Mol. Endocrinol.* **22**, 304–316.

Safe, S., and Wormke, M. (2003). Inhibitory aryl hydrocarbon receptor-estrogen receptor alpha cross-talk and mechanisms of action. *Chem. Res. Toxicol.* **16**, 807–816.

Shanle, E. K., and Xu, W. (2011). Endocrine disrupting chemicals targeting estrogen receptor signaling: identification and mechanisms of action. *Chem. Res. Toxicol.* **24**, 6–19.

Shipley, J. M., and Waxman, D. J. (2006). Aryl hydrocarbon receptor-independent activation of estrogen receptor-dependent transcription by 3-methylcholanthrene. *Toxicol. Appl. Pharmacol.* **213**, 87–97.

Sievers, C. K., Shanle, E. K., Bradfield, C. A., and Xu, W. (2013). Differential action of monohydroxylated polycyclic aromatic hydrocarbons with estrogen receptors alpha and beta. *Toxicol. Sci.* **132**, 359–367.

Soto, A. M., Sonnenschein, C., Chung, K. L., Fernandez, M. F., Olea, N., and Serrano, F. O. (1995). The E-SCREEN assay as a tool to identify estrogens: an update on estrogenic environmental pollutants. *Environ. Health Perspect.* **103**, 113–122.

Swedenborg, E., Ruegg, J., Hillenweck, A., Rehnmark, S., Faulds, M. H., Zalko, D., Pongratz, I., and Pettersson, K. (2008). 3-Methylcholanthrene displays dual effects on estrogen receptor (ER) alpha and ER beta signaling in a cell-type specific fashion. *Mol. Pharmacol.* **73**, 575–586.

Tsai, K. S., Yang, R. S., and Liu, S. H. (2004). Benzo[a]pyrene regulates osteoblast proliferation through an estrogen receptor-related cyclooxygenase-2 pathway. *Chem. Res. Toxicol.* **17**, 679–684.

Van de Wiele, T., Vanhaecke, L., Boeckaert, C., Peru, K., Headley, J., Verstraete, W., and Siciliano, S. (2004). Human colon microbiota transform polycyclic aromatic hydrocarbons to estrogenic metabolites. *Environ. Health Perspect.* **113**, 6–10.

van Lipzig, M. M., Vermeulen, N. P., Gusinu, R., Legler, J., Frank, H., Seidel, A., and Meerman, J. H. (2005). Formation of estrogenic metabolites of benzo[a]pyrene and chrysene by cytochrome P450 activity and their combined and supra-maximal estrogenic activity. *Environ. Toxicol. Pharmacol.* **19**, 41–55.

Vanparys, C., Maras, M., Lenjou, M., Robbens, J., Van Bockstaele, D., Blust, R., and De Coen, W. (2006). Flow cytometric cell cycle analysis allows for rapid screening of estrogenicity in MCF-7 breast cancer cells. *Toxicol. In Vitro* **20**, 1238–1248.

Vondráček, J., Kozubík, A., and Machala, M. (2002). Modulation of estrogen receptor-dependent reporter construct activation and G0/G1-S-phase transition by polycyclic aromatic hydrocarbons in human breast carcinoma MCF-7 cells. *Toxicol. Sci.* **70**, 193–201.

Vondráček, J., Machala, M., Minksová, K., Bláha, L., Murk, A.J., Kozubík, A., Hofmanová, J., Hilscherová, K., Ulrich, R., Ciganek, M., *et al.* (2001). Monitoring river sediments contaminated predominantly with polyaromatic hydrocarbons by chemical and in vitro bioassay techniques. *Environ. Toxicol. Chem.* **20**, 1499–1506.

Vondráček, J., Pěnčíková, K., Neča, J., Ciganek, M., Grycová, A., Dvořák, Z., and Machala, M. (2017). Assessment of the aryl hydrocarbon receptor-mediated activities of polycyclic aromatic hydrocarbons in a human cell-based reporter gene assay. *Environ. Pollut.* **220**, 307–316.

Wihlen, B., Ahmed, S., Inzunza, J., and Matthews, J. (2009). Estrogen receptor subtype- and promoter-specific modulation of aryl hydrocarbon receptor-dependent transcription. *Mol. Cancer Res.* **7**, 977–986.

Xue, W., and Warshawsky, D. (2005). Metabolic activation of polycyclic and heterocyclic aromatic hydrocarbons and DNA damage: a review. *Toxicol. Appl. Pharmacol.* **206**, 73–93.

Zhang, Y., Dong, S., Wang, H., Tao, S., and Kiyama, R. (2016). Biological impact of environmental polycyclic aromatic hydrocarbons (ePAHs) as endocrine disruptors. *Environ. Pollut.* **213**, 809–824.